25th ABCM International Congress of Mechanical Engineering
October 20-25, 2019, Uberlândia, MG, Brazil

# IMPLEMENTATION OF HEAT LOSS MODELING FOR LAMINAR DIFFUSION CH4 FLAMES IN THE FGM METHOD

**Fredherico Nicolaus Rodrigues da Silva**
**Cristian Alex Hoerlle**
Universidade Federal do Rio Grande do Sul, R. Sarmento Leite, 425 - Centro Histórico, Porto Alegre - RS, 90050-170
fredhrsilva@gmail.com, cristian.hoerlle@gmail.com

**André Carlos Contini**
andrecarloscontini@gmail.com
**Fernando Marcelo Pereira**
fernando@mecanica.ufrgs.br

***Abstract.***
*This study aims to implement and explore the inclusion of heat loss in the Flamelet Generated Manifold (FGM) method for the solution of non-premixed laminar methane diffusion flames. The manifold will be generated by taking into account the combustion progress variable, the mixture fraction and heat loss effects modeled through the enthalpy defect technique. In this approach, the manifold is constructed with sets of flamelet solutions employing varying levels of enthalpy defect. This is achieved by, at a first moment, decreasing boundary temperatures, and later by manipulating boundary mixture compositions in the counterflow diffusion flamelets. The adiabatic solution is accounted for an enthalpy defect equal to zero. By having a satisfying number of flamelet sets, the 3D manifold can be constructed and thermochemical data can be retrieved. The steps needed for the generation of flamelets with constant enthalpy defect are described and a reduced manifold is constructed. Results are compared to the detailed solutions employing the DRM19 chemical kinetics mechanism.*

***Keywords:*** *FGM, Enthalpy Defect, Laminar Flow, Diffusion Flames, Non-Adiabatic.*

## 1. INTRODUCTION

Numerical simulation is a powerful tool for helping the development of new and more efficient technologies . On one hand it provides a much less expensive alternative compared to experimental studies, on the other, numerical simulation can be extremely challenging due to limitations in computational power. The reason is that detailed combustion analysis involves a strong coupling of fluid flow with chemical kinetics, which by itself depends on numerous species and chemical reactions.

In recent years the Flamelet Generated Manifold method has been developed as a chemical reduction technique aimed at improving computational times. The manifold is a database where thermochemical data is stored as a function of a given number of control variables. It has been shown that this technique can be used to improve computational time up to a hundred times when compared to the detailed chemical kinetics approaches without a significant loss of accuracy (Van Oijen and de Goey (2000)).

Several studies have been conducted to explore the capabilities, as well as the limitations of the FGM method. For adiabatic laminar diffusion flames, the accuracy and efficiency of the FGM has been shown in recent studies (Verhoeven *et al.* (2012); Zimmer (2016); Hoerlle *et al.* (2017)). Furthermore, non-adiabatic laminar premixed flames have been studied with satisfying results, by taking into account of enthalpy as an additional control variable (Donatti *et al.* (2018)).

To this day, studies on non-adiabatic laminar diffusion flames with the FGM technique are few. In this work we explore the implementation of the enthalpy defect strategy to account for heat losses (Marracino and Lentini (1997)) and discuss some difficulties of the chosen approaches.

## 2. MATHEMATICAL FORMULATION

### 2.1 The Flamelet Generated Manifold

The FGM method is a chemistry reduction technique, based on the idea that a low dimensional subspace, a manifold, composed of several one-dimensional flame structures, called flamelets, can be used to store thermochemical data. Thus, instead of solving all of the transport equations for a reacting flow, which is computationally very demanding, the

CFD code can retrieve any thermochemical variable previously stored in the manifold and resume flow and conservation calculations.

The manifold is constructed by calculating the steady flamelets from a near equilibrium condition up to extinction. One simple way to achieve this is by manipulating the strain rate $a = (-du/dx)_{\rightarrow\infty}$, which describes how stretched a flame is. Extinction is achieved when the strain rate is increased to such lengths ($a \rightarrow \infty$, ie, low residence time within the flame) that reactions can no longer take place. As extinction is achieved and no new steady flamelets can be generated, the manifold can be expanded by including unsteady flamelets that account for increasingly higher values of strain rate. Data is stored as a function of a number of control variables ($CV's$). The control variable is any quantity that can correctly map a dependent variable $\phi$

$$\phi = \phi(CV_1, CV_2, ...CV_n). \tag{1}$$

Figure 1 shows the basic concepts of the FGM methodology. First a set of flamelet solutions is generated and stored. These are used to build the parameterized table (manifold) which stores the thermochemical data. Finally, this data is retrieved from the manifold for subsequent flame calculations.

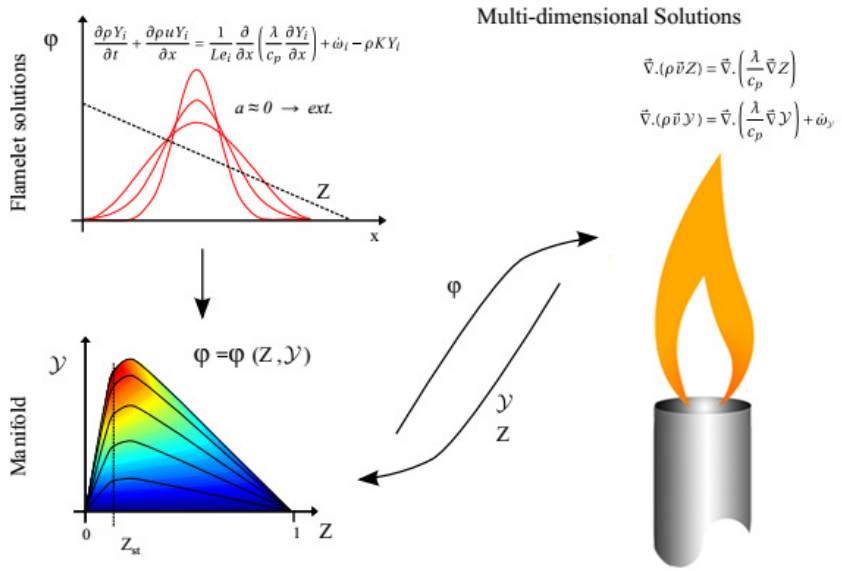


Figure 1: Schematics of the construction of a 2D manifold

The choice of which and how many control variables should be used is not unique. In the case of adiabatic diffusion flames, two $CV's$ are sufficient to correctly represent the thermochemical space. One control variable that is commonly used is the progress variable $\mathcal{Y}$. It can be defined as the combination of mass fractions of certain chemical species such as

$$\mathcal{Y} = \alpha_{CO_2} Y_{CO_2} + \alpha_{H_2O} Y_{H_2O} + \alpha_{H_2} Y_{H_2}, \tag{2}$$

with the weighting factors of the form $\alpha_i = 1/MW_i$.

Another important $CV$ is the mixture fraction $Z$. It relates the amount of mass that originates from the fuel stream to the amount of mass originating from the oxidizer stream. Different formulations for this quantity are available, here we present the one given by Bilger (1989).

$$Z = \frac{Z^* - Z^*_{ox}}{Z^*_{fu} - Z^*_{ox}}, \tag{3}$$

being that for methane we have

$$Z^* = 2\frac{Z_C}{M_C} + \frac{1}{2}\frac{Z_H}{M_H} - \frac{Z_O}{M_O}, \tag{4}$$

where $Z_i$ is the element mass fraction of the element $i$ of mass $M_i$, $fu$ represents they fuel stream and $ox$ the oxidizer stream.

As pointed earlier, in the CFD solution only the conservation of momentum and conservation of mass equations for the control variables need to be solved, as any other quantity can be retrieved directly from the manifold. The conservation for the progress variable and mixture fraction follow as

$$\nabla.(\rho u\mathcal{Y}) = \nabla.\left(\frac{1}{Le_{\mathcal{Y}}}\frac{\lambda}{c_p}\nabla\mathcal{Y}\right) + \dot{w}_{\mathcal{Y}}, \tag{5}$$

$$\nabla.(\rho uZ) = \nabla.\left(\frac{\lambda}{c_p}\nabla Z\right), \tag{6}$$

being $Le_{\mathcal{Y}}$ the Lewis number and $\dot{w}_{\mathcal{Y}}$ the source term for the progress variable which are in turn composed by the Lewis numbers and source terms of the species from which the progress variable is obtained.

The accuracy of the simulations can be improved by adding additional control variables, which increases the manifold size and computational time. This has to be carried out in order to account for heat losses as is described in the next subsection.

### 2.2 Non-Adiabatic Flames

For non-adiabatic reacting flow the combustion progress variable and mixture fraction are no longer sufficient to faithfully parameterize the mass fraction states. Enthalpy now has to be taken into account, more specifically, the enthalpy defect observed along the numerical domain from the adiabatic to the actual state. Marracino and Lentini (1997) define the enthalpy defect $\zeta$ as

$$\zeta = h - (h_{ox} + Z(h_{fu} - h_{ox})), \tag{7}$$

where $h_{ox}$ and $h_{fu}$ represents the enthalpies of the oxidizer and fuel respectively. The term within brackets represents the enthalpy of an adiabatic flame for the same mixture fraction.

Thus, now any thermochemical variable in the reacting flow can be written as

$$\phi = \phi(Z, \mathcal{Y}, \zeta). \tag{8}$$

It is necessary to have different sets of flamelets, each with a given enthalpy defect, for the building of the manifold. Different approaches for achieving enthalpy defect were proposed over the years (Marracino and Lentini (1997); Hossain *et al.* (2001); Messig *et al.* (2013)). Hossain *et al.* (2001) presented the method of calculating counterflow diffusion flames which will be followed in this work. The counterflow flame is illustrated in Figure 2, it consists of two opposing nozzles from which reactants (fuel and oxidant) streams react.

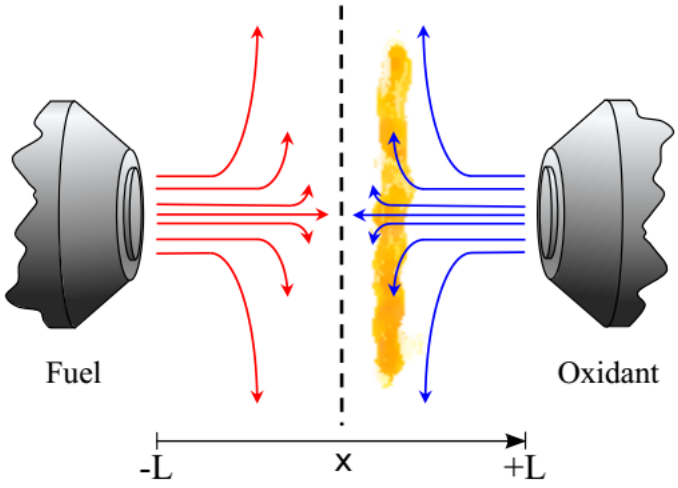


Figure 2: Counterflow Flame

In order to achieve different values of enthalpy defect, the boundary conditions are manipulated in such a way that it causes the enthalpy defect to be constant along the entire domain. The procedure to achieve constant enthalpy defects is only possible to carry out with the limitation of $Le_i = 1$ and is described in the next subsection.

With the inclusion of the enthalpy defect as a new control variable, a new conservation equation has to be solved by the CFD code, this will be the energy equation in terms of the specific enthalpy, and it reads

$$\nabla.(\rho u h) = \nabla.\left(\frac{\lambda}{c_p}\nabla h\right) + \dot{q_R}, \tag{9}$$

where the term $\dot{q_R}$ represents the radiation source term, which can be calculated by several approaches. At this time we assume simply the Optically Thin Approximation (OTA), written as

$$\dot{q_R} = -4\sigma k_p(T^4 - T_\infty^4), \tag{10}$$

being $T_\infty$ the ambient temperature and $k_p$ the mean Planck absorption coefficient, calculated as

$$k_p = \sum_{i=1}^{N_{gg}} p_i k_{p,i}, \tag{11}$$

where $N_{gg}$ is the number of grey-gases, $p_i$ and $k_{p,i}$ are respectively the partial pressure and absorption coefficient for a given species $i$. This model can be further improved, employing discrete ordinates methods for example. From the enthalpy field, calculated by Eq. 9, it is possible to determine the enthalpy defect field, through Eq. 7. Then the enthalpy defect is used to build the 3D manifold.

Finally, the control variables and thermochemical properties are computed and the manifold is constructed. Figure 3 presents the organization of the 3D manifold. This is actually a combination of 2D manifolds (Z and $\mathcal{Y}$ axis), each on its own enthalpy defect level ($\zeta$ axis). Information is retrieved from the spaces between defect levels by interpolation. At the current state, this interpolation method is still being explored.

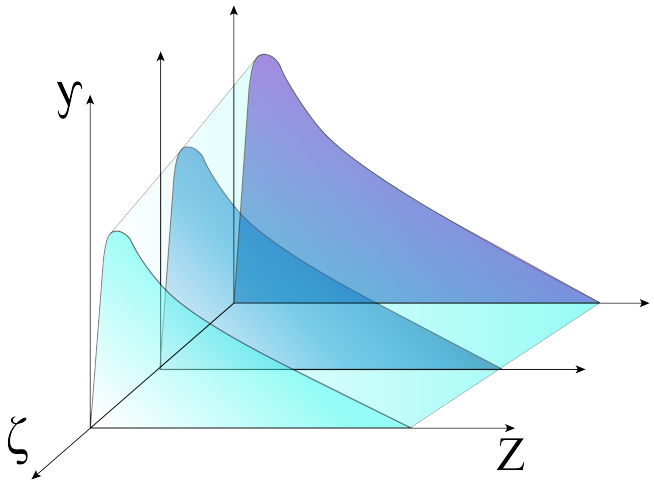


Figure 3: Schematics of the 3D manifold.

### 2.3 Manipulation of the Enthalpy Defect

As stated earlier, the construction of the 3D manifold involves the careful handling of the enthalpy defect as the third control variable. The easiest way to ensure a constant enthalpy defect throughout the entire domain is through control of boundary temperatures. From the transport equations for a reactive flow, the specific enthalpy for a given mixture can be written as the sum of the individual enthalpies as

$$h = \sum_{i=1}^{N_s} Y_i h_i, \tag{12}$$

where

$$h_i = h_{i,f}^0 + \int_{T_{ref}}^{T} c_{p,i}(T)dx. \tag{13}$$

being $Y_i$ and $h_i$ respectively the mass fraction and specific enthalpy for species $i$. The term $h_{i,f}^0$ represents the specific enthalpy of formation for the species $i$ at a temperature $T_{ref}$, and $c_{p,i}$ represents its specific heat. Thus, by manipulating the boundary temperatures, the total enthalpy of the mixture can be controlled. The easiest way for implementing such

control is by changing the temperatures at the boundaries. In this case, since only sensible enthalpy is involved, the enthalpy defect imposed at the boundary is given by

$$\zeta = \Delta h = c_p \Delta T. \tag{14}$$

Following this procedure, Figure 4 a and b show the temperature profiles and enthalpy defects for $\zeta = 0$ (adiabatic flame), $\zeta = -25$ kJ/kg and $\zeta = -50$ kJ/kg along the mixture fraction (Z) axis.

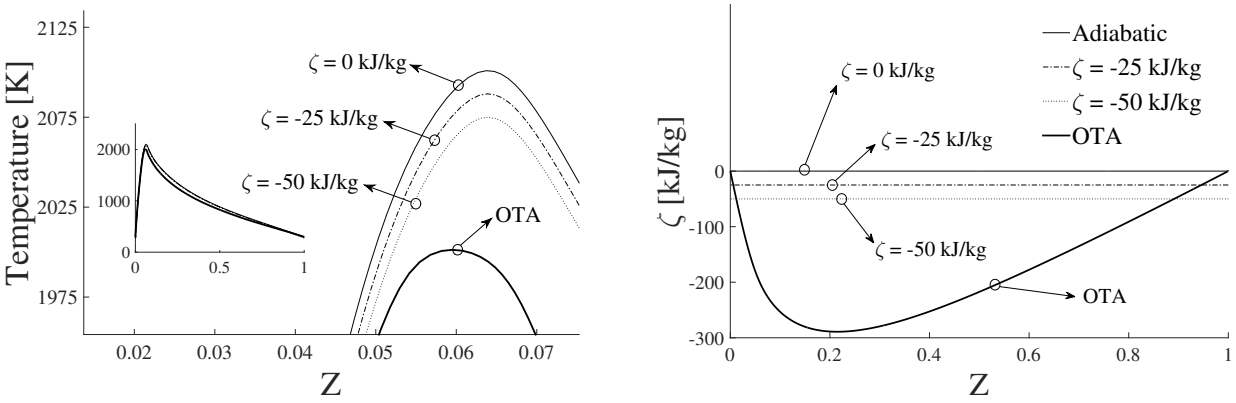


Figure 4: Temperature profiles (a) and enthalpy defects (b) for a strain rate of $a = 10\ s^{-1}$.

The solution for a non-adiabatic flame employing OTA radiation modeling is also presented. Unlike the enthalpy defects obtained through the manipulation of boundary conditions, the OTA enthalpy defect is not constant along the Z axis. In order to map a flame with heat loss, several more levels of enthalpy defect are needed. Preliminary studies show that a total of twelve levels are required for a satisfying representation of the non-adiabatic flame, with decreasing steps of -25 kJ/kg from 0 down to -300 kJ/kg.

Unfortunately, there is a limit for the enthalpy defect levels that can be achieved by simply controlling boundary temperatures. For an enthalpy defect of $\zeta = -50$ kJ/kg the boundary temperature for the oxidant side 248.37 K. Further decreasing this temperature will impact the accuracy of the employed chemical kinetics mechanism. One way to circumvent this and achieve lower enthalpy defects is to manipulate mixture composition.

Figure 5 illustrates how the new composition is obtained for both sides. Starting from the temperature profile of the lowest achieved enthalpy defect, in this case $\zeta = -50$ kJ/kg, the point on the Z axis where this curve crosses the $T = 298$ K ordinate is located. This position sets the new mixture fractions $Z'_{ox}$ and $Z'_{fu}$ for each side.

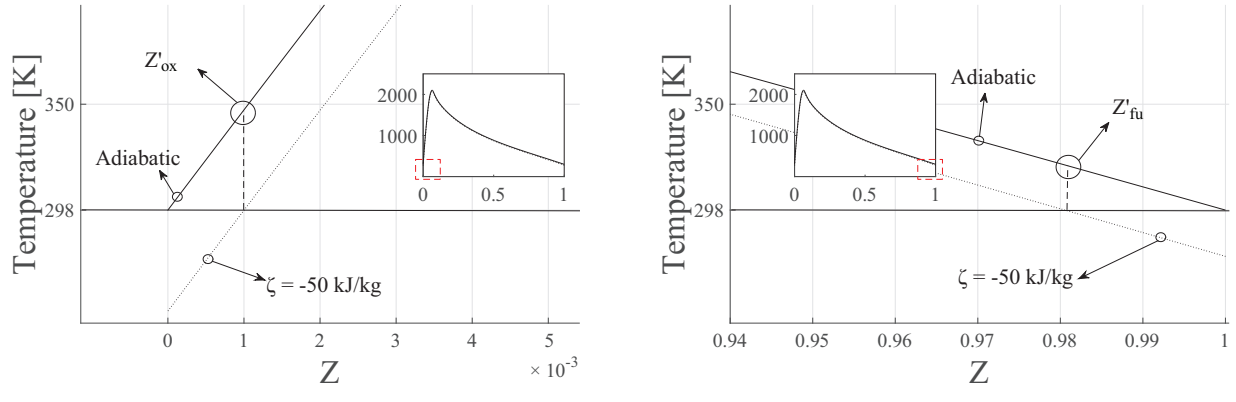


Figure 5: Scheme to obtain new composition for the oxidant side (a) and fuel side (b)

The exact composition of the adiabatic solution at $Z'_{ox}$ and $Z'_{fu}$ is obtained by linear interpolation. This composition is set as a new boundary condition for the new calculations. Equations 12 to 14 tells us that a solution obtained with this composition and at a temperature $T = 298$ K is equivalent to the previous solution for an enthalpy defect of $\zeta = -50$

kJ/kg. In other words, the same defect can be obtained from either manipulating boundary temperatures or composition. As the new mixture fractions are obtained, the Z domain is reduced from 0 to 1 to the new values ($Z'_{ox} = 0.001$ to $Z'_{fu} = 0.981$).

With this in mind, it is now possible to obtain further defect levels by repeating this process. The next two levels of enthalpy defect, $\zeta = -75$ kJ/kg and $\zeta = -100$ kJ/kg are achieved by lowering the temperatures of this new solution. At this point, the same process described in Fig. 3 is repeated, now with the $\zeta = -100$ curve being used to find the new values of Z' on the adiabatic reference profile. From here on all the subsequent defect levels can be obtained by the same method.

Figure 6 shows the mapping of every enthalpy defect level obtained so far. As previously noted, as lower defect levels are obtained a reduction on the Z domain occurs. This effect is more evident at the fuel side of the flame. It can also be observed that although the Z domain is reduced, the OTA curve is always located within these limits.

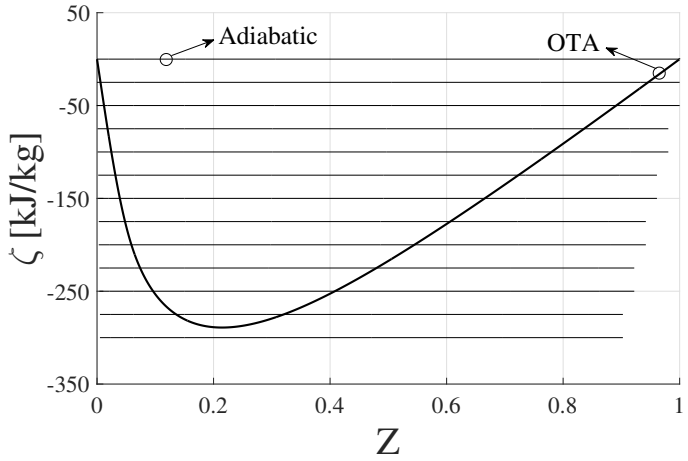


Figure 6: Defect levels needed for mapping heat loss.

## 3. RESULTS

Even though the manipulation of boundary conditions and creation of flamelet solutions are at this point well understood, the creation of the 3D manifold is still proving to be a challenge.

Being that it is much easier to work with enthalpy defects built only with boundary temperature control, the current state of this work explores only this method. For such, a reduced 3D manifold was constructed employing only three levels of enthalpy defect, $\zeta = 0$ kJ/kg, $\zeta = -25$ kJ/kg and $\zeta = -50$ kJ/kg. As this is not sufficient to correctly map the entire radiation effects of the OTA model, the radiation source term was reduced by a factor of $10^{-4}$ in order to minimize radiation effects and keep the OTA enthalpy defect well within the boundaries of the reduced manifold capabilities.

Figures 7 a and b show the preliminary results for temperature profiles for the reduced 3D manifold. The domain has 2.7 cm and 400 grid points. All data from the flamelets is computed, stored and interpolated into a three dimensional grid of dimensions 100 x 50 x 50.

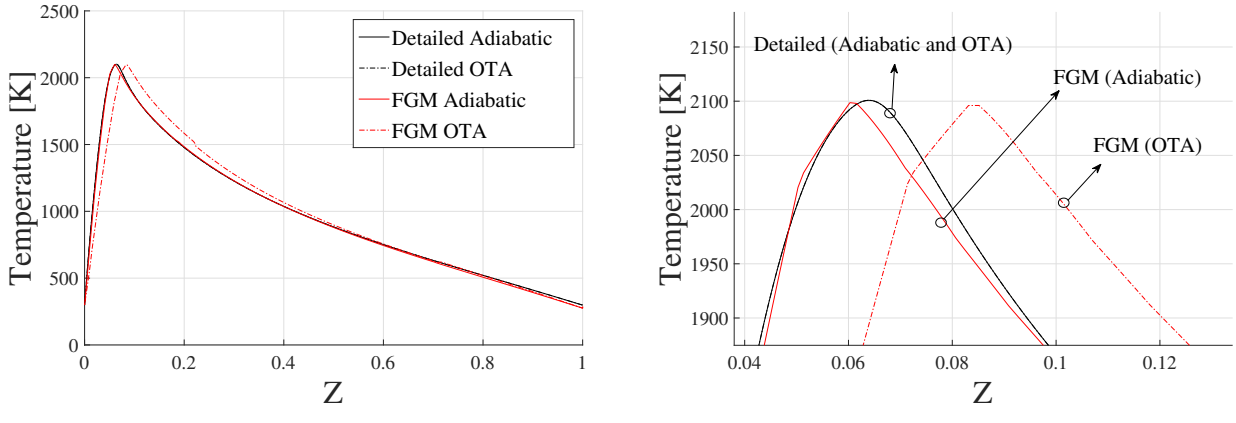


Figure 7: Scheme to obtain new composition for the oxidant side (a) and fuel side (b)

With the reduction of the radiation source term, there is no significant difference between the adiabatic and OTA detailed solutions (both profiles coincide). The adiabatic FGM solution follows closely the detailed solutions. The FGM OTA solution is offset to the fuel side, and as is the case with the detailed solutions, no significant differences are seen for maximum temperature in any profile (being around 2096 K for the FGM OTA solution and 2098 for the others). The reasons for this problems are still being investigated as the authors explore the interpolation algorithms and further implementations needed.

This section is to be expanded as new results are obtained from future development.

## 4. CONCLUSIONS

A reduced three dimensional manifold was constructed with the FGM method employing the already well established mixture fraction and progress variable, as well as the enthalpy defect as control variables, in order to account for heat loss. The enthalpy defect was calculated with the procedure described by Marracino and Lentini (1997) and Hossain *et al.* (2001), with the use of counterflow flamelets and the manipulation of boundary conditions (temperature and mixture composition). The process to achieve constant enthalpy defect levels is thoroughly described.

Results are presented for the reduced manifold, compared to the detailed adiabatic and OTA solutions. The temperature profiles showed significant deviations, which the authors attribute to the limitations of the reduced manifold , as well as to problems in the interpolation procedure.

We are at this moment still investigating ways to implement further interpolation algorithms that will make possible the correct evaluation of non-adiabatic flames, taking into account the full effect of radiation heat loss.

## 5. REFERENCES

Bilger, R.W., 1989. "The structure of turbulent nonpremixed flames". *Symposium (International) on Combustion*, Vol. 22, No. 1, pp. 475–488.

Donatti, L.S., Contini, A.C., Hoerlle, C.A., Zimmer, L., Maders, L. and Pereira, F.M., 2018. "Implementation of the flamelet-generated-manifold for premixed laminar flames with heat loss". In *17th Brazillian Congress of Thermal Sciences and Engineering*. Águas de Lindóia, SP, Brazil.

Hoerlle, C.A., Zimmer, L. and Pereira, F.M., 2017. "Numerical study of co2 effects on laminar non-premixed biogas flames employing a global kinetic mechanism and the flamelet-generated manifold technique". *Fuel*, Vol. 203, pp. 671–685.

Hossain, M., Jones, J.C. and Malalasekera, W., 2001. "Modelling of a bluff-body nonpremixed flame using a coupled radiation/flamelet combustion model". *Flow, Turbulence and Combustion*, Vol. 67, pp. 217–234.

Marracino, B. and Lentini, D., 1997. "Radiation modelling in non-luminous nonpremixed turbulent flames". *Combustion Science and Technology*, Vol. 128, No. 1-6, pp. 23–48.

Messig, D., Hunger, F., Keller, J. and Hasse, C., 2013. "Evaluation of radiation modeling approaches for non-premixed flamelets considering a laminar methane air flame". *Combustion and Flame*, Vol. 160, pp. 251–264.

Van Oijen, J.A. and de Goey, L.P.H., 2000. "Modelling of premixed laminar flames using flamelet-generated manifolds, combustion science and technology". *Combustion Science and Technology*, Vol. 161, No. 1, pp. 113–137.

Verhoeven, L.M., Ramaekers, W.S.J., van Oijen, J.A. and de Goey, L.P.H., 2012. "Modeling non-premixed laminar co-flow flames using flamelet-generated manifolds". *Combustion and Flame*, Vol. 159, pp. 230–241.

Zimmer, L., 2016. *NUMERICAL STUDY OF SOOT FORMATION IN LAMINAR ETHYLENE DIFFUSION FLAMES*. Ph.D. thesis, Universidade Federal do Rio Grande do Sul, Porto Alegre, Brasil.

## 6. RESPONSIBILITY NOTICE

The author(s) is (are) the only responsible for the printed material included in this paper.